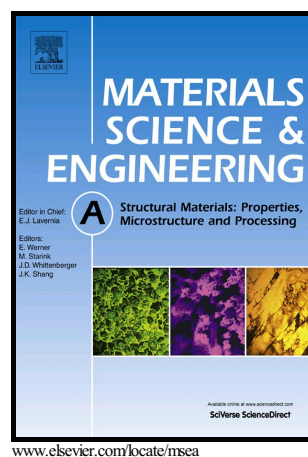


Mechanical behavior and impact toughness of the ultrafine-grained Grade 5 Ti alloy processed by ECAP

I.P. Semenova, A.V. Polyakov, V.V. Polyakova,
Yu.F. Grishina, Yi Huang, R.Z. Valiev, T.G.
Langdon



PII: S0921-5093(17)30543-9
DOI: <http://dx.doi.org/10.1016/j.msea.2017.04.073>
Reference: MSA34974

To appear in: *Materials Science & Engineering A*

Received date: 2 February 2017

Revised date: 4 April 2017

Accepted date: 18 April 2017

Cite this article as: I.P. Semenova, A.V. Polyakov, V.V. Polyakova, Yu.F. Grishina, Yi Huang, R.Z. Valiev and T.G. Langdon, Mechanical behavior and impact toughness of the ultrafine-grained Grade 5 Ti alloy processed by ECAP *Materials Science & Engineering A* <http://dx.doi.org/10.1016/j.msea.2017.04.073>

This is a PDF file of an unedited manuscript that has been accepted for publication. As a service to our customers we are providing this early version of the manuscript. The manuscript will undergo copyediting, typesetting, and review of the resulting galley proof before it is published in its final citable form. Please note that during the production process errors may be discovered which could affect the content, and all legal disclaimers that apply to the journal pertain.

ACCEPTED MANUSCRIPT

Mechanical behavior and impact toughness of the ultrafine-grained Grade 5 Ti alloy processed by ECAP

I.P. Semenova¹, A.V. Polyakov^{2,3*}, V.V. Polyakova¹, Yu.F. Grishina¹, Yi Huang⁴, R.Z. Valiev^{1,3}, T.G. Langdon⁴

¹Ufa State Aviation Technical University, 12 K. Marx street, Ufa, 450008, Russian Federation

²Institute of strategic studies of the Republic of Bashkortostan, 15 Kirova street, Ufa, 450008, Russian Federation

³Laboratory for Mechanics of Bulk Nanostructured Materials, Saint Petersburg State University, 28 Universitetsky pr., 198504, Peterhof, Saint Petersburg, Russian Federation

⁴Materials Research Group, Faculty of Engineering and the Environment, University of Southampton, Southampton, SO17 1BJ, UK

semenova-ip@mail.ru

alex-v.polyakov@mail.ru

vnurik@gmail.com

uliya009@inbox.ru

y.huang@soton.ac.uk

ruslan.valiev@ugatu.su

t.g.langdon@soton.ac.uk

*Corresponding author.

Abstract

This paper reports on a study of the relationship between microstructure, mechanical behavior and impact toughness of the UFG Grade 5 Ti alloy. The mechanical behavior and impact toughness of the Grade 5 Ti alloy in a coarse-grained state, and in an ultrafine-grained (UFG) state produced by equal-channel angular pressing (ECAP) with subsequent deformation-and-thermal treatments via extrusion and warm upsetting in isothermal conditions, were studied extensively. It is shown that a strong refinement of α -grains (less than 250 nm) in the alloy by ECAP and extrusion leads to high strength but with low values of the uniform elongation and lower impact toughness. It is demonstrated that, in order to increase the impact toughness of UFG Ti alloys, it is possible to use approaches realizing ductility enhancement associated with an increase of the strain hardening capacity. An enhancement in the impact toughness of the UFG alloy through an increase in the uniform tensile elongation of the sample is achieved by the preservation of the ultrafine size of α -grains (about 800 nm) with predominantly high-angle

boundaries and a decrease in the dislocation density due to recovery and dynamic recrystallization during warm upsetting.

Keywords: Titanium alloy; ultrafine-grained structure; strength; ductility; uniform elongation; impact toughness.

1. Introduction

Ultrafine-grained (UFG) metals and alloys, produced by various techniques of severe plastic deformation (SPD), exhibit unique mechanical and physical properties [1,2]. It is known that in engineering the strength, ductility and fracture toughness are the most important mechanical properties for the proper mechanical design of structural components. However, UFG metals and alloys often exhibit lower ductility by comparison with their coarse-grained counterparts and this may restrict their application as structural materials in industry. The ductility-related properties relate to characteristics such as the total and uniform tensile elongation, impact toughness and fracture toughness which have a tendency to decrease in metals and alloys subjected to SPD [3].

It has been established that UFG structure formation in titanium and the titanium alloy Ti-6Al-4V makes it possible to attain high values of strength, fatigue endurance limit, superplasticity, etc. [4-6]. Also, a reduction in the size of the α -grains in Ti alloys leads to a decline of ductile properties and impact toughness. For instance, it was shown [7] that the impact toughness with V-notch of UFG Ti produced by ECAP was almost 2 times lower than that of the coarse-grained counterpart. The Ti-6Al-4V alloy with a submicrocrystalline structure produced by multiaxial forging also demonstrates a tendency for decreasing impact toughness [8]. Therefore, finding ways to increase the ductility-related properties, and in particular the impact toughness, of UFG Ti-based materials for advanced engineering applications is a topical problem.

It is well-known that many researchers have associated this with a decline in the strain hardening capacity [3, 9]. At the present time, special attention has been paid to increasing the ductility of UFG metals and alloys through the use of different approaches to UFG structure formation in metals [10]. In particular, it is possible to achieve a combination of high strength and ductility through the formation of a bimodal structure comprised of nanometer- or submicrometer-sized grains and a certain fraction of micrometer-sized grains, where high strength is provided by the ultrafine grains and high ductility is provided by the coarse grains [11]. The nanotwins formed within the ultrafine grains act as barriers for dislocations and

ACCEPTED MANUSCRIPT

facilitate their accumulation in grains, thereby enhancing the strain hardening and ductility of a material [12]. It has been proposed that the introduction of dispersed nanoparticles and segregations into a UFG material may not only lead to the activation of the Orowan strengthening mechanism but may also influence the propagation of shear bands during the deformation where this can have a beneficial effect on the material ductility [13]. The grain shape also plays an important role in the mechanical behavior of UFG metallic materials. In particular, experiments [14] show that a warm caliber rolling treatment of coarse-grained steels with various carbon contents produces a structure consisting of ultrafine ferrite grains of equiaxed shape and dispersed cementite particles having sizes in the range from ~100 to 200 nm. In this case, strengthening is provided by the contribution of the grain-boundary and precipitation mechanisms, while ductility is provided by the ultrafine equiaxed ferrite grains. A similar effect was also observed in the titanium alloy Ti-6Al-4V with a 0.2 wt% B_4C addition which was processed by ECAP [15], where sufficient spherical α - recrystallized grains appeared and the formation of short TiB and TiC whiskers contributed to preventing the micro-cracks as well as crack propagation. As a result, both high strength and elongation were attained.

In the present studies, a new approach was proposed to control strength and ductility, associated with the structure of grain boundaries, where this approach is considered as grain boundary (GB) engineering of UFG metals and alloys [16,17]. In particular, for UFG Ti this approach consisted in increasing of the fraction of high-angle grain boundaries (HAGBs) and it was one of the efficient approaches for raising the work hardening capacity [4, 9, 18]. In this case, an increase in the fraction of HAGBs activates the mechanisms of grain boundary sliding or makes a contribution to work hardening in the process of plastic deformation and, as a consequence, promotes increases in the total and uniform elongations of the sample [18].

Considering the fact that impact toughness also refers to ductility-related properties, one may expect that its value may be connected with ductility characteristics as, for instance, the uniform elongation of a sample under tension. Therefore, approaches producing enhancement of ductile properties can be used to increase the impact toughness of the UFG alloy. In this connection, the aim of the present paper is to study the relationship between microstructure, mechanical behavior and impact toughness of the UFG Grade 5 Ti alloy. In the Grade 5 Ti alloy there are produced two types of UFG structure via ECAP and extrusion with subsequent deformation-and-thermal treatment. The effect of the sharpness of a notch (U, V and fatigue precracked V-notch or T-notch) on the impact toughness of the Ti alloy in the coarse-grained (CG) state and both UFG states was investigated.

2. Material and experimental methods

ACCEPTED MANUSCRIPT

The experiments were conducted using a Grade 5 Ti alloy produced in the form of hot-rolled rods with diameters of 20 mm. The alloy had the following chemical composition (in wt.%): 6.2% Al, 4.3% V, 0.02% Zr, 0.039% Si, 0.16% Fe, 0.06% C, 0.168% O, 0.015% N, 0.003% H, Ti -. Billets with lengths of 100 mm were subjected to heat treatment (HT) which included heating for 1 h to 1143 K with subsequent water quenching and annealing at 948 K for 4 h for a breakdown of martensite [19]. Then the billets were processed by ECAP for 6 passes at 873 K using a die with an angle of 120° between the two channels and processing route B_C in which the sample is rotated around the longitudinal axis by 90° in the same manner between each pass. The rods were then extruded to 12 mm diameter at a temperature of 573 K at which the alloy has the necessary deformation capacity and strengthening via additional grain refining. A final one-hour annealing was imposed at 773 K for reducing the internal elastic stresses without inducing significant growth of the grains [5, 20]. The state produced by ECAP and extrusion will be further referred to as «UFG1».

Then the billets processed by ECAP and extrusion were additionally subjected to forging under isothermal conditions (fig. 1a): the heating temperature of the billet (not more than 20 minutes) and that of the die-set was identical and amounted to 1023 K. The strain accumulated after upsetting was around $\varepsilon \sim 30\%$ and the strain rate did not exceed 10^{-2} s^{-1} . This state is designated as «UFG2».

Cylindrical specimens with a diameter of 3 mm and a gauge length of 15 mm were used for the tensile tests. The scheme of cutting of specimens from the billets is shown in fig. 1b. The tensile testing was performed at an initial strain rate of $1 \times 10^{-3} \text{ s}^{-1}$ at room temperature on an Instron testing machine.

Notched samples were machined from the CG/UFG billets along their deformation direction according to the Russian standard GOST 9454-78 with a U, V and T-notch (with an induced fatigue crack). Samples with a cross-section of $5 \times 10 \text{ mm}$ were cut out from the billets according to the scheme presented in fig. 1a. The samples were tested using a Charpy impact tester with an impact energy of 50 J at an impact velocity of 3.85 m s^{-1} .

The microstructures of samples were analyzed by transmission electron microscopy (TEM). Samples for foils were cut out using electrical discharge machining, mechanically thinned to a thickness of 100 μm and then electro-polished using a TenuPol-5 facility with a solution of 5% perchloric acid, 35% butanol and 60% methanol, at a polishing temperature within the range from -20 to $-35 \text{ }^{\circ}\text{C}$. The microstructures were examined using a JEOL JEM 2100 microscope operating with an accelerating voltage of 200 kV. The size of the α -phase grains was estimated from dark-field TEM and SEM images of the microstructure by averaging

the diameters of more than 300 grains and/or subgrains. The volume fraction of the primary α -phase grains was estimated by a secant linear method.

X-ray diffraction analysis was conducted on a Rigaku Ultima IV diffractometer. The samples were examined with CuK α -radiation (40kV, 30 mA, the slit size was 2-10 mm). The phase composition of the alloy was determined via the Rietveld refinement method using the MAUD (Material Analysis Using Diffraction) software [21]. Concerning the values determined for the phase volume fractions, the weighted profile R-factor (Rwp) was added to indicate their reliability [22]. The measurement error was 2%. The surface fracture features after testing were examined using a JEOL JSM 6390 scanning electron microscope (SEM).

3. Results

3.1. Microstructure of Grade 5 Ti before and after HT+ECAP+extrusion

Figure 2a displays the SEM image of the alloy microstructure in the as-received state (Fig. 2a). The microstructure consists of grains of the primary α -phase with a size of $8 \pm 2 \mu\text{m}$ in the transverse section (fig. 1a) and $10 \pm 2 \mu\text{m}$ in the longitudinal section (fig. 2b) of the billet, having a volume fraction of $\sim 65\%$ and a β -transformed lamellar structure. It can be seen from the TEM images of the $\alpha+\beta$ region (fig. 2c) that the average width of the secondary α -phase plates was $\sim 1 \mu\text{m}$.

Figure 3 shows typical microstructures of the alloy after HT+ECAP+extrusion – UFG1. In fig. 3a it can be seen that the fraction of the primary α -phase grains does not exceed 25% as a result of the preliminary HT. Their size is $6 \pm 2 \mu\text{m}$ in the transverse section. In the longitudinal sections of billets, the primary α -phase grains have a strongly elongated shape with a length of up to $25 \mu\text{m}$ (fig. 3b). As a result of severe plastic deformation, in the bodies of α -grains there is observed an increase in the dislocation density with the formation of weakly misoriented substructures of a cellular type (fig. 3c). Figure 3d shows regions having refined α - and β -grains, with an equiaxed shape. The average grain size for the α - and β -phases is $\sim 350 \text{ nm}$.

Fig. 4 shows the X-ray patterns of the as-received and UFG1 samples of the Grade 5 alloy, which include a set of the main X-ray peaks corresponding to α -Ti (hcp lattice) and β -Ti (fcc lattice). In the X-ray pattern of the UFG sample (fig. 4 b) many peaks are significantly broadened, to the extent of merging with the level of the diffuse-scattering background, which is conditioned by high internal stresses associated with a heavy distortion of the crystalline lattice. The UFG1 sample is characterized by a high dislocation density (up to $4.7 \times 10^{15} \text{ m}^{-2}$). According to X-ray analysis, the volume fraction of the α -phase was increased after this treatment from 85 to 94%. A decrease in the fraction of the metastable β -phase is explained by

an active $\beta_m \rightarrow \alpha + \beta$ transformation induced by SPD processing; it should be noted that this was also reported earlier [23].

Figure 5 shows the microstructure of the Grade 5 Ti alloy in the UFG2 state produced by HT+ECAP+extrusion and additional isothermal upsetting. The SEM images of the microstructure reveal a more isotropic microstructure in the transverse and longitudinal sections of the billets (fig. 4a). The UFG2 microstructure in the TEM images is represented by equiaxed recrystallized and deformed grains of the α -phase with a mean size of 0.8 μm (fig. 5b). The total dislocation density is much lower at about 10^{14} m^{-2} . On the basis of the X-ray phase analysis, the volume fraction of the β -phase in comparison with the state after HT+ECAP+extrusion has increased from 6 to 10% as a result of the deformation temperature increase to 1023 K.

3.2. Mechanical properties of the Grade 5 Ti alloy in the coarse-grained, UFG1 and UFG2 states

Fig. 6 shows typical tensile curves for the samples from the CG, UFG1 and UFG2 states of the alloy. Fig. 5 and Table 1 demonstrate that the ultimate tensile strength of the alloy in the UFG1 state is ~1435 MPa on average, and this is almost 45% higher than that of the CG alloy (UTS \approx 965 MPa) due to α -grains refinement. The total elongation to failure of the samples is 9% on average and it is noticeably lower than in the initial as-received state (17%). It should also be noted that there is a marked decrease in the uniform elongation value to 1.7% in the UFG1 sample. As demonstrated by many studies, strain localization in SPD-processed materials is often observed under both monotonic and cyclic deformation this provides the nuclei for subsequent fracture [24]. In the samples with the UFG2 structure there is observed a decline in strength to 1220 MPa as compared to the UFG1 state of 1435 MPa (Table 1). At the same time, the ductility visibly grows and in particular the uniform and total elongations increase to 9 and 16%, respectively. It is evident that the decline in ultimate tensile strength can be accounted for, in the first place, by grain growth (from 0.35 to 0.8 μm) resulting from the processes of dynamic recrystallization and recovery occurring in the course of isothermal upsetting. The increase in the elongation to failure of the samples is conditioned by a marked decrease in dislocation density. In addition, the increase in the volume fraction of the β -phase in the structure after warm upsetting from 6 to 10% (see section 2.3) also makes an additional contribution to the enhancement of the alloy ductility. The shape of the tensile curve of the samples with the UFG2 structure indicates an increased capacity of the material for strain hardening, which is characterized by a substantial increase in uniform elongation in comparison with the UFG1 state.

Table 1. Mechanical properties of the Grade 5 Ti samples at room temperature in various structural states.

	State	UTS, MPa	0.2 YS, MPa	Elong., %	Uniform elong., %
1	As-received	965±10	900±20	17±1	8.5±0,2
2	UFG1	1435±10	1360±40	9±1	1.7±0,3
3	UFG2	1220±5	1180±10	16,0±0,3	9.0±0,2

3.3. Impact toughness of the samples with U, V and T-notches

Table 2 presents the results of impact tests of the samples with different types of microstructure and notches. It is apparent that in all the structural states of the alloy, an increase in the notch sharpness (U, V and T) reduces impact toughness. For example, for the alloy initial CG state, the KCT value is more than 2 times smaller than the KCU value (0.61 and 0.23 MJ/m², respectively). From Table 2 it can be seen that for the UFG1 and UFG2 states of the alloy this difference between KCU and KCT is slightly larger.

Table 2. Impact toughness of the Grade 5 Ti alloy in different structural states.

Impact toughness, MJ/m ²	CG (8.0 µm)	UFG1 (0.3 µm)	UFG2 (0.8 µm)
KCU	0.61±0.05	0.33±0.03	0.42±0.02
KCV	0.54±0.02	0.15±0.01	0.32±0.01
KCT	0.23±0.02	0.11±0.01	0.18±0.02

Fig. 7 shows the dependence of impact toughness on the offset yield strength 0.2%YS for the Grade 5 Ti alloy with different types of microstructure. The common tendency of decline in impact toughness with increasing strength of the alloy is maintained for all the states. It is visible from the diagram shown in fig. 6 that for KCU the decline in impact toughness is more intensive than for KCT, i.e. for the samples with the highest notch sharpness.

The decline in the impact toughness of the Grade 5 Ti alloy during the transition from the CG state to the UFG1 state is quite predictable and is related primarily to a high sensitivity to strain localization. Such a behavior of the alloy is apparent from the tensile curve (fig. 5) where the uniform elongation of the UFG1 alloy is below 2%, i.e. almost 4 times smaller than the uniform elongation of the CG alloy (8%). The sample with the UFG2 structure has an intermediate position in terms of strength and impact toughness, its ultimate tensile strength

being visibly higher than that of the CG alloy (1220 and 950 MPa, respectively), but lower than that of the alloy with the UFG1 structure, having the highest UTS of 1435 MPa. Accordingly, it is apparent that for UFG2 a noticeable increase in uniform elongation up to 9% has resulted in a significant enhancement in impact toughness with different notch shapes (table 2 and fig. 7).

3.4. Fractography

The fracture surfaces of the samples from the CG alloy, as well as those of the samples with the UFG1 and UFG2 microstructures, have a homogeneous structure, which is evidence of the macro-ductile character of the fracture. The SEM images of the fracture surface are characterized by a dimple microrelief but also some differences are observed related to the features of the alloy microstructure (fig. 8). In the case of fracture in the CG alloy, the microrelief consists of comparatively large (in size $\sim 5 \mu\text{m}$) and deep, slightly elongated dimples, where this is typical of conventional CG Ti alloys (fig. 8a). In the samples with a microstructure of the UFG1 type, dimples are finer and have an equiaxed shape, but their size is non-uniform. Thus, there are individual large dimples up to $5 \mu\text{m}$ in size, commensurable with the quantity of the primary α -phase, and very small dimples below $1 \mu\text{m}$ in size, the fraction of the latter being much larger, which may indicate a predominantly intercrystalline character of fracture (fig. 8b). The samples in the UFG2 state in the fracture have rather large (up to $10 \mu\text{m}$) and elongated dimples with smoother surface in comparison with the UFG1 state (fig. 8c). There are also typical signs indicating the alloy micro-ductile fracture and an intercrystalline and transcrystalline character of the crack fracture is present as in the CG samples.

4 Discussion

The results of the present study demonstrate the typical features of mechanical behavior of the Grade 5 Ti alloy in the CG state and in the UFG1 state produced by HT+ECAP+extrusion. A reduction in the size of grains/subgrains of the α - and β -phases to $0.3 \mu\text{m}$ led to a considerable, almost 1.5-fold, increase in yield strength, which is in agreement with the well-known Hall-Petch relationship [25]. The ultimate tensile strength of the alloy reached 1435 MPa, whereas the strength of the conventional Ti-6Al-4V alloy normally does not exceed 1000 MPa. As is known, the thermomechanical treatment by extrusion that followed after ECAP promoted the elongation of grains, the formation of a developed substructure in the grains, a considerable dislocation accumulation, which increases the contribution of the dislocation and texture mechanisms of

strengthening, together with the grain boundary mechanism [26]. This approach for CP Ti [6, 26] and for Ti-6Al-4V alloy [6, 19] was used successfully.

At the same time, the tensile curves of the UFG samples exhibited early strain localization under tension and a decrease in the uniform elongation value from 8.5 to 1.7 %. This is conditioned by the fact that in UFG metals under the conditions of very small grains (below 1 μm) the nucleation of new dislocations and their accumulation is hampered, which may lead to early strain localization and fracture [23]. This effect is associated with such microstructural features as a high, almost critical, dislocation density ($4.7 \times 10^{15} \text{ m}^{-2}$), the formation of substructures in the interior of elongated grains, and high internal stresses which hinder the nucleation of new dislocations and their accumulation [27]. Such features are typical for metallic materials subjected to SPD which often leads to early strain localization and fracture [24, 27]. In addition, note should be made that SPD processing initiates the $\beta \rightarrow \alpha$ phase transformation, which leads to an increase in the fraction of the harder α -phase from 85 to 94%, and, consequently a decrease in the total ductility of the alloy. Evidently, it can be expected that the above-mentioned features of the UFG Grade 5 alloy will contribute to a reduction in the fracture toughness and impact toughness.

The impact toughness of samples with the UFG1 structure is also almost 2 times lower than the impact toughness in the initial CG state, which apparently can also be accounted for by the features of the UFG structure formed by SPD processing [28]. It is evident that in UFG materials, in contrast to CG materials, there are more potential sites for the generation of pores and nanocracks, which is conditioned by the predominant dislocation nucleation at grain boundaries [29] as well as by the high density of grain boundaries and triple joints at which the formation of nanocracks and pores takes place [30, 31]. On the whole, this contributes to the realization of predominantly intergranular (intercrystalline) fracture character, independent of the crack propagation mechanisms by micro-ductile or de-cohesion failure [3]. This can be seen well in fig. 7b showing the fracture surface relief of the sample with the UFG1 structure, where the dimple size is almost commensurable with the sizes of grains/subgrains of the α and β -phases.

In the present study, in order to raise the ductility and impact toughness of the UFG Grade 5 Ti alloy produced by HT+ECAP followed by extrusion, an additional deformation-and-thermal treatment (warm upsetting in isothermal conditions) was used. This type of treatment at a temperature of 1023 K, on the one hand, enabled preserving the ultrafine range of grains (0.8 μm) and on the other hand the boundaries of deformed and new recrystallized grains had predominantly high-angle misorientations, as evidenced by the TEM images of the structure (fig.3). Moreover, recovery processes at the given deformation temperature resulted in a reduction in the total dislocation density and internal elastic stresses. Such structural changes

contributed to the enhancement in the alloy capacity for work hardening and therefore to an increase in the uniform elongation value of the samples from 1.7% in the UFG1 state to 9.0% in the UFG2 state. In this state, the ultimate tensile strength decreased from 1435 to 1220 MPa due to grain growth from 0.3 to 0.8 μm , but its level remained noticeably higher than in the as-received state (965 MPa). The total elongation and the uniform elongation were practically the same as in the CG sample (table 1). The impact toughness of the alloy in the UFG2 state also increased considerably from 0.15 to 0.32 MJ/m^2 . This can evidently be accounted for by several reasons: first, a decrease in the total density of dislocations and internal elastic stresses which increase the area of plastic deformation at the top of a crack [8]. Besides, after the upsetting the shape of the α -phase grains changed and transformed from an elongated shape to an equiaxed shape due to the dynamic recrystallization process during the upsetting, with the size of the ultrafine grains growing slightly, on average, from 0.3 to 0.8 μm . In addition, an increase in the volume fraction of grains of the soft β -phase in the two-phase structure (from 6 to 11%) also makes an additional contribution into the growth of the alloy ductility. Such microstructural transformations were observed in the UFG Ti-6Al-4V alloy after tension at elevated temperatures, when the samples exhibited increased values of uniform elongation, retaining high strength [32]. Attention has been drawn to the important role of the equiaxed shape of the α -phase grains in the composite titanium alloy T18 with 0.2 wt% B₄C addition, which facilitates ductile fracture [15]. The role of second phases is played here by the shorter TiB and TiC fibers that can prevent the micro-cracks as well as crack propagation, thereby improving the sample ductility and toughness [15].

In addition, it is important to note that in this study with the UFG Grade 5 alloy the grain boundaries became more equilibrium with a predominantly high-angle misorientation as a result of dislocation redistribution in the process of recovery [33]. It is known that high-angle grain boundaries (HAGBs) in UFG metals and alloys are more efficient in terms of strengthening, as compared to low-angle grain boundaries [16, 33]. Moreover, HAGBs can have a positive effect on toughening mechanisms as well. In particular, in an interstitial-free steel it was demonstrated that, as compared with LAGBs, the HAGBs were more effective in strengthening and toughening of the steels [34]. Therefore, refined grains with a large volume fraction of HAGBs (≈ 60 pct) effectively increase the absorbed energy even at room temperature by slowing the fracture propagation [35].

Fig. 9 shows the available data for the offset yield strength and the impact toughness KCV for Ti and some other Ti alloys. It is readily apparent that Grade 5 Ti in the as-received CG state has a rather high impact toughness ($\text{KCV} = 0.54 \text{ MJ/m}^2$), but a relatively low yield strength ($0.2\text{YS} = 900 \text{ MPa}$). The conventional heat treatment permits an increase in yield strength (to

950 MPa) but reduces impact toughness ($KCV = 0.42 \text{ MJ/m}^2$) (fig. 8). As was shown earlier [8], the formation of a homogeneous submicrocrystalline (SMC) structure in the Ti-6Al-4V alloy by multiaxial forging leads to a substantial increase in yield strength to 1200 MPa and a decline in impact toughness to 0.18 MJ/m^2 . For the UFG alloy produced by HT+ECAP+extrusion (in the present study, referred to as the UFG1 state), yield strength and the impact toughness KCV were 1360 MPa and 0.23 MJ/m^2 , respectively. A similar result was obtained in the earlier study [8], where the formation of a bimodal SMC structure in the alloy enabled a somewhat increasing impact toughness to 0.24 MJ/m^2 while preserving a rather high ductility ($0.2YS = 1355 \text{ MPa}$). In the present study, an increase in the uniform elongation (from 1.7 to 8%) and impact toughness (from 0.17 to 0.32 MJ/m^2) of the Grade 5 Ti alloy samples, subjected to warm isothermal upsetting after SPD processing, was achieved concurrently with some decline in strength (1220 MPa).

Thus, in order to increase the impact toughness of UFG Ti alloys, it is possible to use approaches realizing ductility enhancement, in particular due to the formation of a specific UFG structure design ensuring, for example, a bimodal size distribution of grains, a predominantly equiaxed shape, an increase in the fracture of HAGBS in the structure and a non-equilibrium degree of the boundaries. In the present investigation, it is demonstrated that in the Grade 5 Ti alloy the formation of ultrafine grains of α - and β -phases, having a predominantly equiaxed shape, with equilibrium boundaries and high-angle misorientation, enables an increase in the strain hardening capacity and hence ductility and impact toughness. Also, some decline in strength due to grain growth is observed. At the same time, it appears that there is a potential for attaining higher values of strength and impact toughness for the UFG Grade 5 Ti alloy by varying the sizes and shapes of α and β -phase grains, the state of the grain boundaries, as well as by controlling the morphology and distribution of dispersed secondary phases and segregations. These approaches will be used in our future investigation of the fracture toughness K_{IC} which is one of the most important engineering properties of structural materials.

Conclusions

In the Grade 5 Ti alloy, a UFG structure was produced by ECAP followed by deformation-and-thermal treatments via extrusion and warm isothermal upsetting, ensuring a good balance of high strength, ductility and impact toughness. From the results of the research, the following conclusions are made:

1. The formation, in the Grade 5 Ti alloy, of a UFG structure with a mean α -grain size of $0.35 \mu\text{m}$ leads to a high strength of 1435 MPa, but at the same time to a reduction in the total and

uniform elongation (9 and 1.7%) in comparison with the same characteristics of the CG alloy (950 MPa, 17 and 8%, respectively).

2. It is shown that the increase in yield strength and the reduction in uniform elongation in the UFG alloy reduce the impact toughness of the samples with different notch sharpness (U, V and T) almost by 2 times.
3. The ultrafine-grained structure consisting of equiaxed α -grains, with a mean size of 0.8 μm , having high-angle misorientations and a reduced dislocation density as a result of the processes of recovery and dynamic recrystallization occurring during isothermal upsetting, leads to an increase in the total and uniform elongation and to an increase in the impact toughness as well.

Acknowledgements

The work described in sections 2, 3.1 and 3.2 was conducted with the support of the Russian Science Foundation under grant No. 16-19-10356 in USATU, and the work described in sections 3.3 and 3.4 was supported by the RFBR grant No. 16-58-10061. The work of two authors was supported by the European Research Council under ERC Grant Agreement No. 267464-SPDMETALS (YH and TGL).

References

- [1] R.Z. Valiev, Y. Estrin, Z. Horita, T.G. Langdon, M.J. Zehetbauer, Y.T. Zhu, Producing Bulk Ultrafine-Grained Materials by Severe Plastic Deformation, JOM 58 (2006) 33–39. doi:10.1007/s11837-006-0213-7
- [2] R.Z. Valiev, Y. Estrin, Z. Horita, T.G. Langdon, M.J. Zehetbauer, Y.T. Zhu, Fundamentals of superior properties in bulk nanoSPD materials, Mater. Res. Lett. 4 (2016) 1–21. doi:10.1080/21663831.2015.1060543
- [3] R. Pippan, A. Hohenwarter, The importance of fracture toughness in ultrafine and nanocrystalline bulk materials, Mater. Res. Lett. 4 (2016) 127–136. doi:10.1080/21663831.2016.1166403
- [4] A.V. Polyakov, I.P. Semenova, R.Z. Valiev, Y. Huang, T.G. Langdon, Influence of annealing on ductility of ultrafine-grained titanium processed by equal-channel angular pressing-Conform and drawing, MRS Commun. 3 (2013) 249 - 253. doi:10.1557/mrc.2013.40
- [5] A.V. Polyakov, I.P. Semenova, Y. Huang, R.Z. Valiev, T.G. Langdon, Fatigue Life and Failure Characteristics of an Ultrafine-Grained Ti–6Al–4V Alloy Processed by ECAP and Extrusion, Adv. Eng. Mater. 16 (2014) 1038–1043. doi:10.1002/adem.201300530

- [6] I.P. Semenova, G.I. Raab, R.Z. Valiev, Nanostructured titanium alloys: New developments and application prospects, *Nanotechnologies in Russia* 9 (2014) 311-324. doi:10.1134/S199507801403015X
- [7] I. Sabirov, R.Z. Valiev, R. Pippan, About application of three dimensional analyses of fracture surfaces in fracture study on nanostructured titanium, *Computational Materials Science* 76 (2013) 72–79. doi:10.1016/j.commatsci.2012.12.027
- [8] S.V. Zherebtsov, Strength and ductility-related properties of ultrafine grained two-phase titanium alloy produced by warm multiaxial forging, *Mater. Sci. Eng. A* 536 (2012) 190-196. doi:10.1016/j.msea.2011.12.102
- [9] R.Z. Valiev, A.V. Sergueeva, A.K. Mukherjee, The effect of annealing on tensile deformation behavior of nanostructured SPD titanium, *Scr. Mater.* 49 (2003) 669–674.
- [10] I.A. Ovid'ko and T.G. Langdon, Enhanced ductility of nanocrystalline and ultrafine-grained metals, *Rev. Adv. Mater. Sci.* 30 (2012) 103-111.
- [11] Y. Wang, M. Chen, F. Zhou, E. Ma, High tensile ductility in a nanostructured metal *Nature* 419 (2002) 912-915. doi:10.1038/nature01133
- [12] E. Ma, Y. M. Wang, Q.H. Lu, M.L. Sui, L. Lu, K. Lu, Strain hardening and large tensile elongation in ultrahigh-strength nano-twinned copper, *Applied Physics Letters* 85 (2004) 4932-4934. doi:10.1063/1.1814431
- [13] C.C. Koch, Optimization of strength and ductility in nanocrystalline and ultra-fine grained metals, *Scripta Mater.* 49 (2003) 657-662. doi:10.1016/S1359-6462(03)00394-4
- [14] S. Torizuka, E. Muramatsu, S.V.S.N. Murty and K. Nagai, Microstructure evolution and strength-reduction in area balance of ultrafine-grained steels processed by warm caliber rolling, *Scr. Mater.* 55 (2006) 751. doi:10.1016/j.scriptamat.2006.03.067
- [15] L. Wang, X. Wang, L.Ch. Zhang, W. Lu, Ultrafine processing of (TiB+TiC)/TC18 composites processed by ECAP via Bc route, *Materials Science and Engineering: A* 645 (2015) 99-108. doi: 10.1016/j.msea.2015.08.011
- [16] R.Z. Valiev, On grain boundary engineering of UFG metals and alloys for enhancing their properties, *Materials Science Forum* 584-586 (2008) 22-28. doi:10.4028/www.scientific.net/MSF.584-586.22
- [17] Y.H. Zhao, J.F. Bingert, Y.T. Zhu, X.Z. Liao, R.Z. Valiev, Z. Horita, T.G. Langdon, Y.Z. Zhou and E.J. Lavernia, Tougher Ultrafine-Grain Cu via High-Angle Grain Boundaries and Low Dislocation Density, *Appl. Phys. Lett.* 92 (2008) 081903(1-3). doi:10.1063/1.2870014
- [18] I.P. Semenova, G.H. Salimgareeva, G.Da Costa, W. Lefebvre, R.Z. Valiev, Enhanced strength and ductility of ultra-fine grained Ti processed by severe plastic deformation, *Advanced Engineering Materials* 12 (2010) 803-807 doi:10.1002/adem.201000059.

- [19] I.P. Semenova, A.V. Polyakov, V.V. Polyakova, Y. Huang, R.Z. Valiev and T.G. Langdon, High-Cycle Fatigue Behavior of an Ultrafine-Grained Ti-6Al-4V Alloy Processed by ECAP and Extrusion, *Adv. Eng. Mater.* 18 (2016) 2057-2062. doi:10.1002/adem.201500630
- [20] I.P. Semenova, E. B. Yakushina, V.V. Nurgaleeva, R.Z. Valiev, Nanostructuring of Ti-alloys by SPD processing to achieve superior fatigue properties, *International Journal Materials Research* 100 (2009) 1691-1696. doi: 10.3139/146.110234
- [21] P. Scardi, L. Lutterotti, R. Di Maggio, Size-Strain and quantitative phase analysis by the Rietveld method, *Adv. X Ray Anal.* 35A (1992) 69-76.
- [22] B.H. Toby, R factors in Rietveld analysis: How good is good enough?, *Powder Diffr.* 21 (2006) 67. doi:10.1154/1.2179804
- [23] I.P. Semenova, L.R. Saitova, R.K. Islamgaliev, T.V. Dotsenko, A.R. Kil'mametov, S.L. Demakov, R.Z. Valiev, Evolution of the structure of the VT6 alloy subjected to equal-channel angular pressing, *The Physics of Metals and Metallography* 100 (2005) 66-72.
- [24] A.Yu. Vinogradov, S.R. Agnew, Fatigue of Nanocrystalline Materials, in: *Encyclopedia of Nanoscience and Nanotechnology*, Marcel-Dekker, New York, USA, 2004, pp. 2269-2288.
- [25] Hall-Petch G.E. Dieter, D. Bacon, *Mechanical metallurgy*, SI Metric ed., McGraw-Hill, New York, 1986.
- [26] V.V. Stolyarov, Y.T. Zhu, T.C. Lowe, R.K. Islamgaliev, R.Z. Valiev, A Two step SPD processing of ultrafine-grained titanium, *Nanostructured Materials* 11 (1999) 947-954. doi: 10.1016/S0965-9773(99)00384-0
- [27] E. Ma. Eight routes to improve the tensile ductility of bulk nanostructured materials and alloys, *JOM* 58 (2006) 49-53. doi:10.1007/s11837-006-0215-5
- [28] R.Z. Valiev, Nanostructuring of metals by severe plastic deformation for advanced properties, *Nature Materials* 3 (2004) 511-516. doi:10.1038/nmat1180
- [29] X. Huang, N. Hansen, N. Tsuji, Hardening by annealing and softening by deformation in nanostructured metals, *Science* 312 (2006) 249-251. doi:10.1126/science.1124268
- [30] D. Farkas, S. Van Petegem, P.M. Derlet, H. Van Swygenhoven, Dislocation activity and nano-void formation near crack tips in nanocrystalline Ni, *Acta Mater.* 53 (2005) 3115-3123.
- [31] K.S. Kumar, S. Suresh, M.F. Chisholm, J.A. Horton, P. Wang, Deformation of electrodeposited nanocrystalline nickel, *Acta Mater.* 51 (2003) 387-405. doi: 10.1016/S1359-6454(02)00421-4
- [32] A.V. Sergueeva, V.V. Stolyarov, R.Z. Valiev, A.K. Mukherjee, Superplastic behavior of ultrafine-grained a Ti-6Al-4V alloys, *Materials Science and Engineering A323* (2002) 318-325.

- ACCEPTED MANUSCRIPT
- [33] R.Z. Valiev, M.Yu. Murashkin, I.P. Semenova, Grain boundaries and mechanical properties of ultrafine-grained metals, *Metall. Mater. Trans. A* 41 (2010) 816-822. doi:10.1007/s11661-009-0083-z
- [34] Onur Saray, Gencaga Purcek, Ibrahim Karaman, Hans J. Maier, Impact Toughness of Ultrafine-Grained Interstitial-Free Steel, *Metallurgical and Materials Transactions A* 43 (2012) 4320–4330. doi:10.1007/s11661-012-1238-x
- [35] Ming-Chun Zhao, Xiao-Fang Huang, Jing-Li Li, Tian-Yi Zeng, Ying-Chao Zhao, Andrej Atrens, Strength and toughness tradeoffs for an ultrafine-grain size ferrite/cementite steel produced by warm-rolling and annealing, *Mater. Sci. Eng. A* 528 (2011) 8157–8168. doi: 10.1016/j.msea.2011.07.067

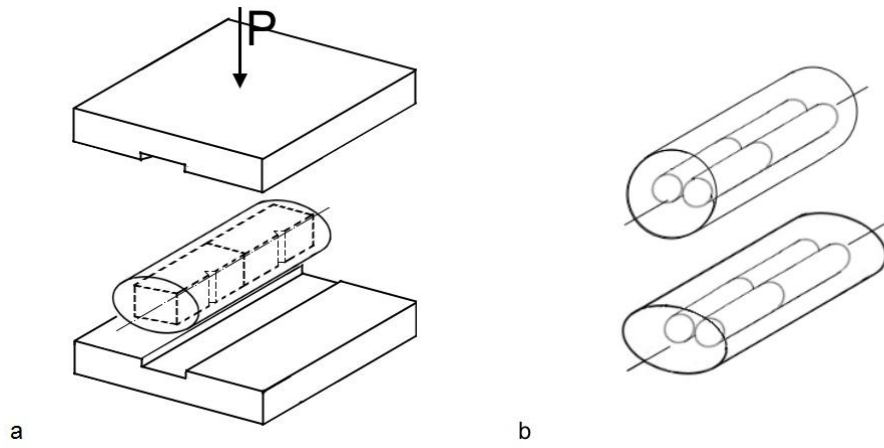


Fig. 1. Forging scheme (a) and cutting scheme of an impact bending samples (a) and tensile samples (b) for the UFG Grade 5 Ti billets.

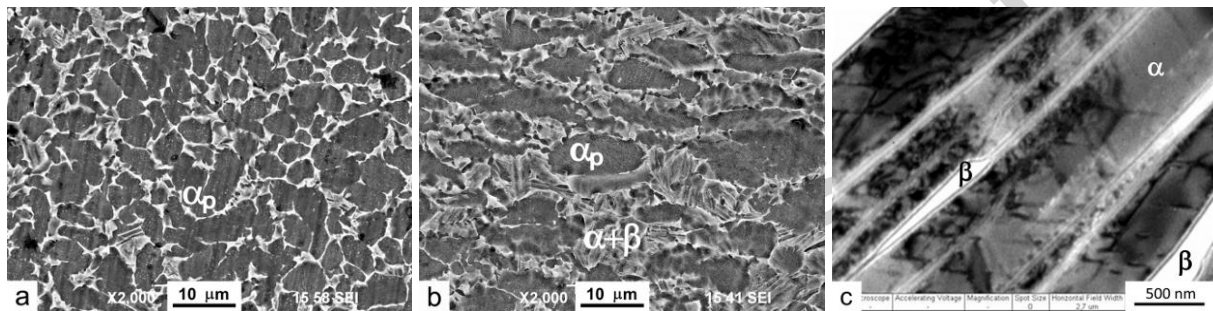


Fig. 2. View of the duplex (globular-plate) microstructure of as-received Ti Grade 5 alloy: (a) SEM image of the microstructure of the billet's transverse section; (b) SEM image of the microstructure of the billet's longitudinal section; (c) typical $(\alpha+\beta)$ plate structure field (e.g. in fig. b) on the TEM image at high magnification.

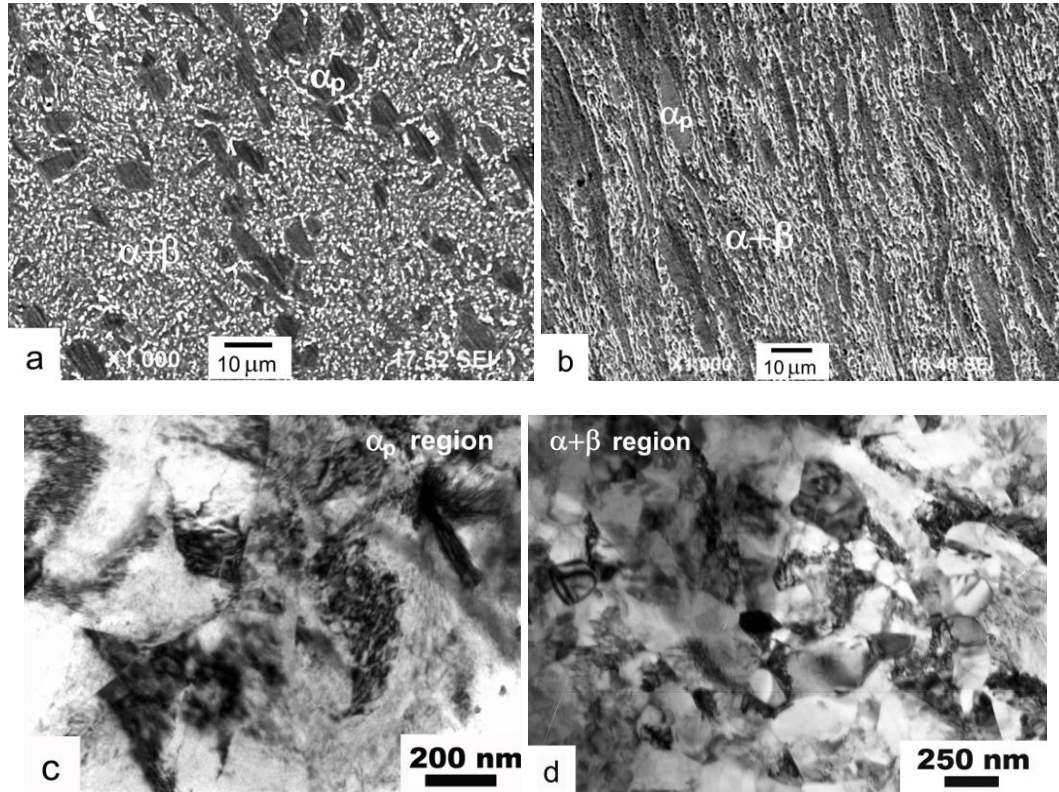


Fig. 3. The microstructure of the Ti Grade 5 alloy after ECAP and extrusion (state UFG1): (a) SEM image of the microstructure of the billet transverse section; (b) SEM image of the microstructure of the billet longitudinal section; (c) fragmented grains of the α_p phase; (d) TEM image of the UFG ($\alpha + \beta$) structure.

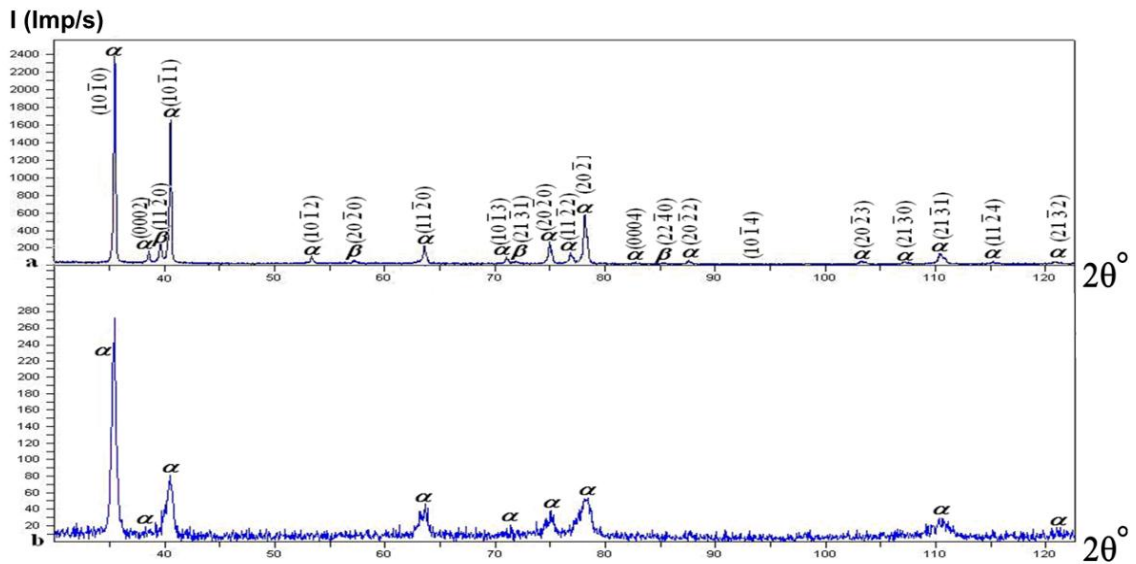


Fig. 4. The X-ray diagram of Grade 5 Ti with CG (a), UFG1 (b) and UFG2 (c) structure.

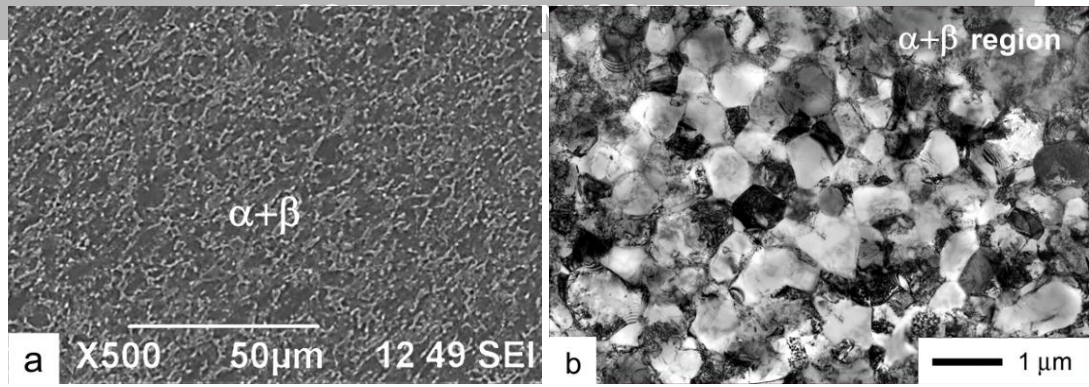


Fig. 5. The microstructure of the Ti Grade 5 alloy subjected SPD processing by ECAP + extrusion and isothermal forging at 1023K: (a) SEM image of the structure of the billet's transverse and longitudinal sections; (b) TEM image of the microstructure.

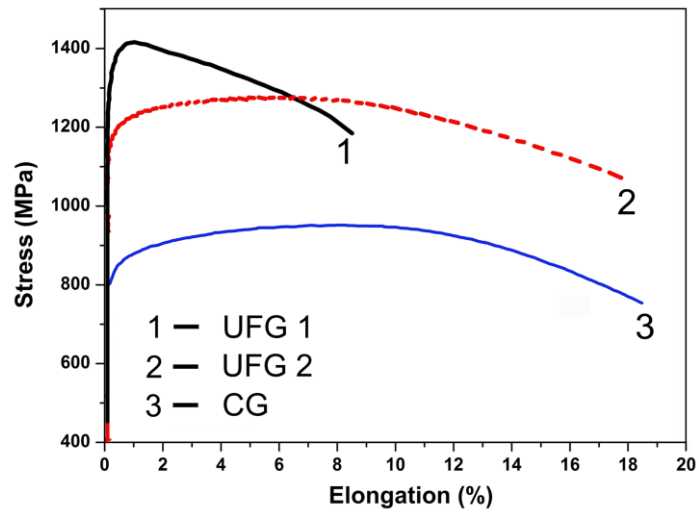


Fig. 6. Typical tensile curves of Ti Grade 5 samples with CG, UFG1 and UFG2 structure.

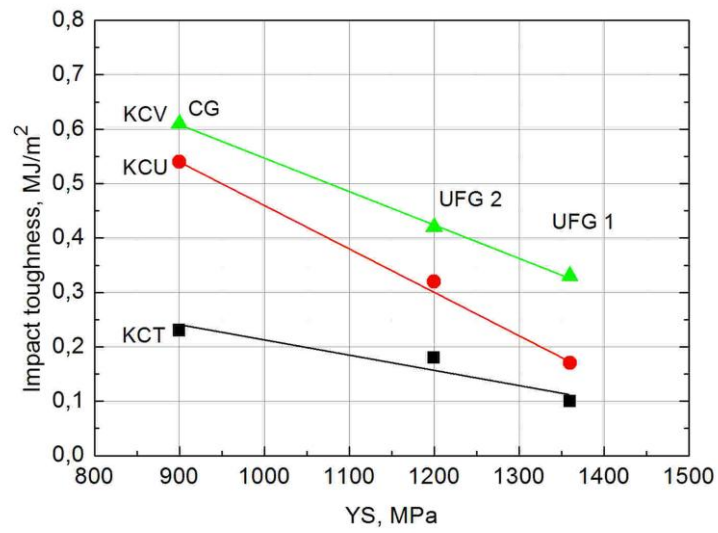


Fig. 7. The dependence of impact toughness values KCU, KCV and KCT on 0.2 YS of Ti Grade 5 alloy with CG, UFG1 and UFG2 structure.

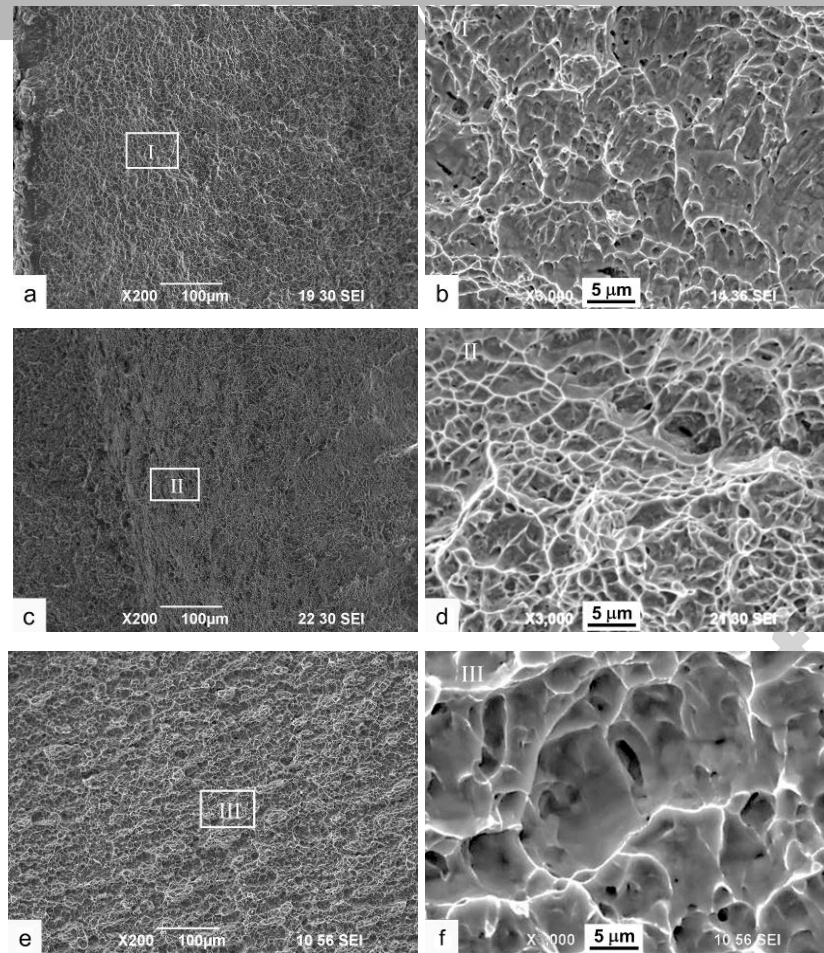


Fig. 8. SEM images of the sample fracture surfaces after the impact toughness test: (a), (b) – CG state; (c), (d) – UFG1 state; (e), (f) – UFG2 state.

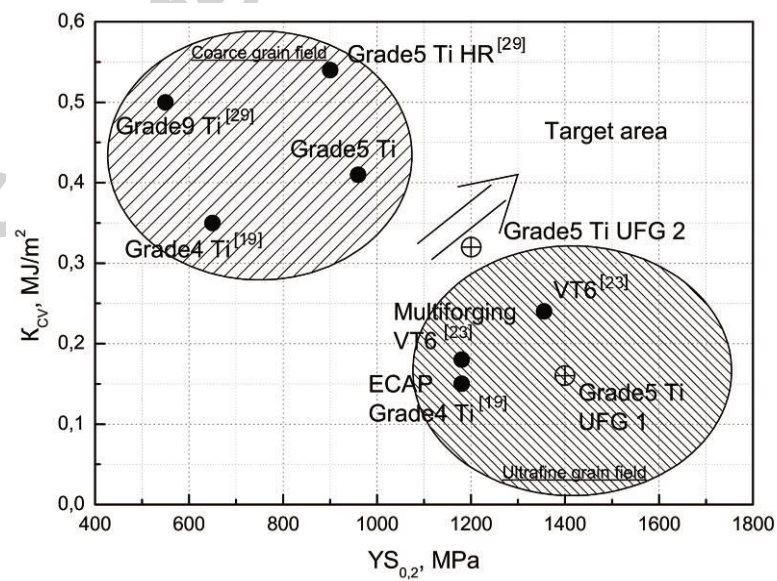


Fig. 9. The dependence between 0.2 YS and the impact toughness KCV for Ti and its alloys.